



New design to remove leukocytes from platelet-rich plasma (PRP) based on cell dimension rather than density

Subhaini Jakfar^{a,b}, Tzu-Chieh Lin^a, Shinn-Chih Wu^c, Yao-Horng Wang^d, Yu-Jun Sun^a, Minal Thacker^a, Li-Xin Liu^e, Feng-Huei Lin^{a,f,*}

^a Institute of Biomedical Engineering, National Taiwan University, Taipei, 106, Taiwan

^b Dentistry Faculty, Syiah Kuala University, Darussalam, 23111, Banda Aceh, Indonesia

^c Department of Animal Science and Technology, National Taiwan University, Taipei, Taiwan

^d Department of Nursing, Yuanpei University of Medical Technology, 306, Yuanpei Street, Hsinchu, 300, Taiwan

^e School of Materials Science and Engineering, Center of Functional Biomaterials, Key Laboratory of Polymeric Composite Materials and Functional Materials of Education, GD Research Center for Functional Biomaterials Engineering and Technology, Sun Yat-Sen University, Guangzhou, 510275, China

^f Institute of Biomedical Engineering and Nanomedicine, National Health Research Institutes, Miaoli, 350, Taiwan

ARTICLE INFO

Keywords:

Platelet-rich plasma (PRP)
Filtered-tube design
Homemade design
Cut-off pore size
Platelets
Growth factors

ABSTRACT

Platelet-rich plasma (PRP) can stimulate the proliferation of stem cells and have a positive effect on tissue repair. Although many commercialized PRP preparation kits are already on the market, first-line clinical workers are still not satisfied with most of the PRP kits. The work of commercial PRP kits is based on the density of blood elements. However, the blood elements are very close in density which makes the separation challenging. Therefore, the mentioned commercialized kits are generally contaminated by leukocytes and erythrocyte. In this study, a home-designed PRP device was developed to use a separation membrane with adequate cut-off pore size of 5 μm , 3 μm and 2 μm for the groups of H5M, H3M, and H2M, respectively, to be placed in the middle of the centrifuge tube. The home-designed H2M showed a very promising results regardless of the final volume (1.82 ± 0.09 ml), platelet yield ($8.39 \pm 0.44\%$), Red Blood Cells (0%), White Blood Cells (0%), and Relative Concentration of Platelet Increment value (225.09%). Further, it showed a good result in cell viability and cytotoxicity and confirmed a good multilineage potentials. The concentration in PRP prepared by group H2M was relatively stable and far above average. All the fibrin fibers were linked together as bridging strands or strings and turned into an inter-connected porous structure for nutrients transportation and regenerative cell migration. We believe that the home-designed group H2M should have a great potential to develop into the final product to meet the requirements of first-line clinical workers.

1. Introduction

Fibrin glue and fibrin sealant have been applied for medical treatments as hemostatics, tissue sealant, and tissue adhesive during surgery since the early 1980s [1,2]. However, fibrin glue or fibrin sealant was not so extensively used in tissue repair or regeneration due to limited growth factors in concentration [3,4]. Platelet-rich plasma (PRP) that contains a buffy coat and is rich in platelets and growth factors was introduced in 1997 by Whitman et al. to have a better effect on tissue repair, especially in bone, cartilage, skin, dental alveolar tissue and even as a drug/cell carrier for controlled release [5,6].

PRP is a blood plasma containing higher-than-baseline levels of platelets [7]. It can be activated by adding thrombin and/or calcium chloride (CaCl_2) wherein it will release the growth factors from alpha granules like fibroblast growth factor-2 (FGF-2), transforming growth factor-beta 1 (TGF- β 1), bone morphogenic growth factor-2 (BMP2), insulin-like growth factors 1 (IGF1), platelet-derived growth factor (PDGF), and the other cytokines [8–11]. Those are valuable in stimulating, signaling, and promoting cells to involve in tissue repair process [12–15]. The varieties of up-to-date commercial PRP kits are available on the market, however, each shows a different predominance in the final products, for instance, the number of harvested platelets, the

Peer review under responsibility of KeAi Communications Co., Ltd.

* Corresponding author. Institute of Biomedical Engineering, National Taiwan University, Taipei, 106, Taiwan.

E-mail address: double@ntu.edu.tw (F.-H. Lin).

<https://doi.org/10.1016/j.bioactmat.2021.03.002>

Received 20 January 2021; Received in revised form 21 February 2021; Accepted 2 March 2021

2452-199X/© 2021 The Authors. Publishing services by Elsevier B.V. on behalf of KeAi Communications Co. Ltd. This is an open access article under the CC

BY-NC-ND license (<http://creativecommons.org/licenses/by-nc-nd/4.0/>).

percentage of leukocytes or erythrocytes, the final volume PRP, price and operation time [7,11,15]. Many commercialized PRP preparation kits on the market follow the protocol as they did in fibrin glue preparation; that might result in less plasma volume, limited platelet number, too many leukocyte/erythrocytes and inadequate fibrin ultra-structure [11,16,17]. Currently, several new PRP devices or kits coming to the market generally have more user-friendly protocols than before. Even though the first-line clinical workers are still not satisfied with most of the currently available PRP kits, no matter in a final volume of PRP, platelet number, the concentration of growth factors, the number of leukocytes/erythrocytes, or fibrin ultra-structure.

The commercialized PRP kits can be divided into two categories: plasma-based kits and buffy coat-based kits [7,18]. Collecting platelets from whole blood by the centrifugation process through the conventional way brings the whole blood into three layers: (1) the plasma layer on the top is about 55% of whole blood and is the least dense component, (2) the buffy coat remains in the middle which is less than 1% of whole blood and is very rich in leucocytes & platelets, (3) the erythrocytes rest at the bottom and are about 45% of whole blood [16]. The plasma-based kits harvest only the top plasma layer which contains fewer platelets; in contrast, the buffy coat kits harvest both the plasma layer and buffy coat which has a higher concentration of platelets, as it is called the platelet-rich plasma (PRP). The platelets can release more growth factors to induce local cells or mesenchymal stem cells to join the repair processes during tissue healing; this means the buffy coat kits show more improvement when used in tissue repair or regeneration [19,20]. Nevertheless, in some cases the leucocytes containing in PRP as found in buffy coat layer might induce deleterious effect to bone regeneration by increasing pro-inflammatory cytokines, or platelet might also induce fibrosis by stimulating extracellular matrix production [21,22]. Further, a dose-dependent manner of PRP occurs to the cell respond in which the limitation of the cell membrane receptors may be counterproductive of cell function when the growth factors released by platelet too high [23]. The work of the commercial buffy coat kits available today are commonly based on blood-component density [24,25]. However, the blood elements are very close in density which makes the separation of blood elements a challenge if only traditional centrifugation is used. Therefore, the aforementioned commercialized buffy coat kits are generally contaminated by leucocytes that would induce local inflammation and deteriorate the healing process, or additionally, filtration by erythrocyte might lead to local cells necrosis [21,26,27]. In addition, the number of granulocytes in PRPs would interfere with the formation of the fibrin ultra-structure, such as the fibrin diameter, pore size and porosity etc., that may be related to cell migration during the healing process [28].

On the other hand, membrane filtration technology has rapidly developed. As a result, various membrane products are widely used in applications such as in food and beverage processes, pharmaceutical and medical applications, chemical processing, water, wastewater treatment, and other purification applications. Those membranes can be classified based on processes, materials, configuration, or performs. The track-etched membrane filter is one sort of membrane manufacturing process. The film is exposed in a nuclear reactor containing charged particles bombards on the film surface, leaving behind sensitized tracks. Continued with treating the membrane with etching agent such as NaOH, then this surfactant-doped alkaline solution will produce more homogeneous pore geometry. The membrane materials commonly used are polycarbonate (PCT) or polyester (PET). Polycarbonate track-etched (PCTE) membrane has successfully applied in blood plasma separation with other blood cells [29,30], besides for use in many industrial areas, as aforementioned.

In this study, a new device was designed to prepare PRP based on the size of blood elements, instead of density, in an attempt to yield PRP with relatively high platelet number, less contamination of erythrocytes/leukocytes, an optimum level of growth factors, and high final volume. As known, each of the blood elements has a large difference in

diameter; for instance, a platelet is around 2–3 μm , an erythrocyte is about 6–9 μm and a leukocyte is approximately 6–19 μm [31–34]. If a membrane with the proper pore size stays in the middle of a centrifuge tube to serve as a filter, we could easily separate the platelet and plasma from the erythrocyte & leukocytes. However, erythrocytes are fragile and due to the shear stress, might be damaged during the centrifugation process, thus leading to contamination [35–37]. This study used a two-step process after harvesting whole blood from a donor through a blood sample tube. First, the process of centrifugation is carried out in order to sedimentation the erythrocyte to the bottom of the centrifuge tube, and then the bottom layer is discarded, and the buffy coat and plasma are transferred to the home-designed tube with a membrane being placed in the middle of the tube with the purpose of separating leukocytes from the final PRP product. Through this two-step method and use of the membrane, we could obtain high quality and very purified PRP as a source or feed material for tissue repair. The PRP product from this design can be compared to the other commercial kits in terms of final volume, level of growth factors, number of platelets, number of erythrocytes & leukocytes, and fibrin ultra-structure etc. Furthermore, we also evaluated the cell viability of the cell exposed to the prepared PRPs by WST-1 assay and Live/Dead stain. The healing ability of PRPs can be confirmed by the stemness of porcine bone marrow stem cells (PBMSCs), such as osteogenesis, chondrogenesis and adipogenesis, with the techniques of histo-immuno staining and gene expression.

2. Materials and methods

2.1. The tube designed to prepare PRP

As described previously, the PRP harvest is carried out in a two-step process. Firstly, whole blood is harvested through a blood sample tube and then is given the first centrifugation (Kubota 5010 centrifuge, Japan) to separate out the erythrocytes. Secondly, the bottom layer is discarded, the buffy coat & plasma are transferred to the home-designed tube fitted with a membrane filter with different cut-off pore size of 5 μm , 3 μm and 2 μm (PCTE, Sterlitech Corp, USA) settings in the middle of the tube, which separates the leukocytes from the final PRP. The whole scheme to prepare PRP using this home-designed tube is shown in Fig. 1. Involving animals or animal tissue parts of this experiment were performed accordingly to the guidelines determined by the Institutional Animal Care and Use Committee (IACUC) of Pigmodel Animal Technology Co.,Ltd (IACUC Approval Number PIG-108030, approved on December 16, 2018).

2.2. The membrane characterization

To evaluate the membranes used in the study, structure and actual pore size of the membranes have been examined under the scanning electron microscope (Jeol, JSM-7800F Prime, Japan) with an accelerating voltage of 15 kV.

2.3. Platelet-rich plasma preparation

A total volume of 500 ml of whole blood was harvested from a swine by an internal jugular veni-puncture with a 20-gauge needle supplemented with ACD-A anticoagulant (GBiosciences, USA). The blood sample was divided into eight groups to prepare PRP according to different protocols or designs, as described in Table 1.

2.4. Complete blood count

The concentration of the blood components which included platelets, white blood cells, and red blood cells from whole blood and PRPs were measured at National Taiwan University Hospital, Taipei, Taiwan, by using an automated veterinary hematology analyzer (IDEXX ProCyte Dx) for a complete blood count (CBC).

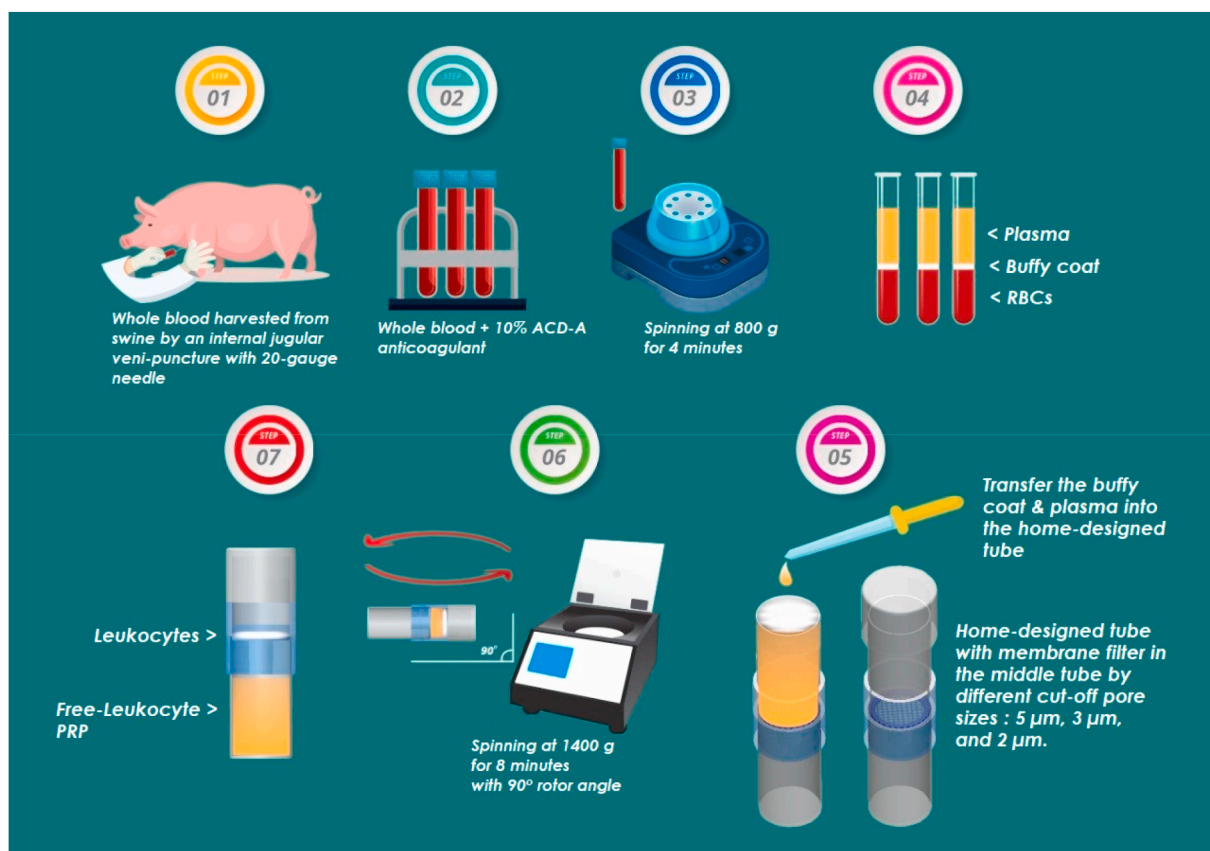


Fig. 1. The scheme of design and operation for the home-design tube.

Table 2 summarizes the formulae for the counting and evaluation of all the blood cellular components [38].

2.5. Platelet-rich plasma activation

The PRP from all groups was activated by using 23 mM CaCl_2 and then was centrifuged at 180 g-force for 3 min, and then remained overnight at 4–8 °C. The supernatant was harvested and stored at –80 °C for later-on experiments.

2.6. Growth factors quantification

The growth factors quantification of PRPs including fibroblast growth factor-2 (FGF-2), transforming growth factor-beta 1 (TGF-β1), bone morphogenetic protein-2 (BMP-2) and insulin-like growth factor-1 (IGF-1) were quantified by using ELISA kits according to the user instructions, with product number SEA050Po, SEA013Po, SEA124Po, and CEA551Po, respectively, from Wuhan USCN Business. Co., Ltd., USA.

2.7. Cell viability test using primary porcine chondrocyte

In this study, the WST-1 and Live/Dead stain were used to evaluate the cell viability of the prepared PRPs using primary cultured porcine chondrocyte. The procedures are briefly described as follows.

The hyaline cartilage was harvested from porcine knee joints, scraped using a scalpel, and cut into small pieces in PBS. Subsequently, the pieces were washed in PBS containing PSA antibiotics (Sigma Aldrich), and following that they soaked in 0.25% trypsin solution, and then stayed in the incubator for 30 min. The cartilage pieces were further digested with 0.2% collagenase (in DMEM-HG with 10% FBS) for 16 h and then washed with 1x PBS to isolate the chondrocytes from the pieces. The isolated chondrocytes were further washed with PBS and

centrifuged. Finally, using DMEM-HG supplemented with 10% FBS and added 1% PSA, the cells later expanded by monolayer culture in the incubator at 37 °C and 5% CO_2 .

Chondrocyte proliferation is the analysis of the number of viable cells, based on colorimetric quantification by using tetrazolium salt WST-1 through mitochondria dehydrogenase in viable cells. In brief, the primary chondrocytes were seeded into a 96-well plate with a density of 5000 cells per well on average. After being left to culture for 1 day, the chondrocytes were fully attached on the plate ground. The medium was changed by using medium of 90% DMEM-HG mixed with 10% PRPs. The PRPs would be prepared from the 8 groups as marked on Table 1. Zinc diethyldithiocarbamate (ZDEC) and alumina (Al_2O_3) would be used as the positive control and negative control, respectively. After 24 h, the medium was refreshed by the WST-1 working solution, 100 μl per well, and cultured for another 2 h. The plate was mounted onto the ELISA reader to measure cell viability by absorbance spectrum at 450 nm.

The different colour of fluorescence generated from living cells and dead cells in either culture conditions or experimental treatments reflects the condition of cell viability, apoptosis, and necrosis. Living cells are identified in intracellular esterase activity (green fluorescence), while dead cells shown by the lack of esterase activity, and non-intact plasma membrane are identified by red dye staining. In brief, the primary chondrocyte cells were seeded in 24-well plate with a density of 4×10^4 cells per well by using a DMEM-HG medium for 24 h. For the next 24 h, the previous medium was discarded and refreshed with the experimental mediums (DMEM-HG + 10% PRPs). On the third day, the cells were stained for 30 min with two mixing solutions: 2 μM calcein AM (Thermo Fisher, Waltham, MA, USA) for live cell staining; and 4 μM ethidium homodimer-1 (Thermo Fisher) for dead cells staining. Finally, a confocal microscope (FV300 Confocal Laser Scanning Microscope, Olympus) was used to observe cell survival.

Table 1
PRPs used in the study and Abbreviation.

Group	Abbreviation	Description
Whole Blood	WB	The whole blood directly harvested from a donor
Conventional protocol	CP-PRP	The whole blood was harvested from a donor and go one-round centrifugation by 800 g force turns whole blood into three layers. The top two layers were obtained to prepare PRP through a syringe. The final product is called CP-PRP.
Tube inserted with 5 μ m filter	H5M	CP-PRP was obtained from the previous method and then transferred to a home-designed tube with a membrane cut-off pore size of 5 μ m being set in the middle of the tube. The tube is placed in a centrifuge; and then the leukocytes are further filtered out by 1400 g force from the final PRP product that is the group called H5M.
Tube inserted with 3 μ m filter	H3M	CP-PRP was obtained from the previous method and then transferred to a home-designed tube with a membrane cut-off pore size of 3 μ m which is set in the middle of the tube. The tube is placed in a centrifuge; and then the leukocytes are further filtered out by 1400 g force from the final PRP product that is the group called H3M.
Tube inserted with 2 μ m filter	H2M	CP-PRP was obtained from the previous method and then transferred to a home-designed tube with a membrane cut-off pore size of 2 μ m which is set in the middle of the tube. The tube is placed in a centrifuge; and then the leukocytes are further filtered out by 1400 g force from the final PRP product that is the group called H2M.
Vegas Biotech PRP kit	VB	Commercialized PRP kit from Senzen Vegas Biotech
Acti-PRP kit	AP	Commercialized PRP kit from Aeon Biotherapeutic
Sanli PRP kit	SL	Commercialized PRP kit from Sanli
Manson PRP kit	MS	Commercialized PRP kit from Manson

Table 2
Formula to characterize the cellular components.

A. Volume Yield (VY%) = $\frac{\text{volume of product(ml)}}{\text{volume of WB processed(ml)}} \times 100$
B. Platelet Yield (PY%) = $\frac{\text{volume of product(ml)} \times \text{Platelet concentration in product (x10}^9 \text{/}\mu\text{L)}}{\text{volume of WB collected(ml)} \times \text{Platelet concentration in WB (x10}^9 \text{/}\mu\text{L)}} \times 100$
C. RBC Yield (RY%) = $\frac{\text{volume of product(ml)} \times \text{RBC concentration in product (x10}^9 \text{/L)}}{\text{volume of WB collected(ml)} \times \text{RBC concentration in WB (x10}^9 \text{/L)}} \times 100$
D. WBC Yield (WY%) = $\frac{\text{volume of product(ml)} \times \text{WBC concentration in product (x10}^9 \text{/L)}}{\text{volume of WB collected(ml)} \times \text{WBC concentration in WB (x10}^9 \text{/L)}} \times 100$
E. Relative Concentration of Platelets (RCP%) = $\frac{\text{Platelet concentration in product (x10}^9 \text{/L)}}{(\text{Platelet (x10}^9 \text{/L)} + \text{WBC (x10}^9 \text{/L)} + \text{RBC (x10}^9 \text{/L)}) \text{ from WB}} \times 100$
F. Relative Concentration of Platelet Increment (RCPI%) = $\frac{\text{RCP of Product (\%)}}{\text{Baseline RCP of WB (\%)}} \times 100$

2.8. The examination of fibrin network structure under SEM

The scanning electron microscope (SEM) was used to examine the fibrin ultra-structure of the prepared PRPs. The prepared PRPs were activated by calcium chloride and immediately dropped onto a silicon wafer with a size of 5 \times 5 mm by a pipette tip; and then placed in a refrigerator at 5 $^{\circ}$ C for 10 min for coagulation or gel formation. The coagulated PRPs were fixed in 2% glutaraldehyde in Dulbecco's phosphate buffer saline (DPBS) buffer overnight. It was then washed 3 times in a phosphate buffer/50% EtOH each time for 15 min. The specimens were then transferred to buffered osmium tetroxide for post-fixation for

1 h. The process continued with the specimens being washed in a phosphate buffer for 5 min, then dehydrated in series alcohol of 30%, 50%, 70%, 85%, 90%, 95%, and two times with 100% ethanol (30 min for each step), after which the samples were dried completely in a critical point dryer (CPD). The sample was mounted to the Al sample stage of SEM and then surface coated with a platinum film by a sputtering PVD. The fibrin ultra-structure of the coagulated and fully fixed PRPs was examined under a scanning electron microscope (Jeol, JSM-7800F Prime, Japan) with an accelerating voltage of 15 kV.

2.9. The immunophenotyping of PBMSCs

The porcine bone marrow stem cells (PBMSCs) were directly obtained from the Lab of Transgenic Animal, Department of Animal Science & Technology, National Taiwan University, which is supervised by Prof. SC Wu. The PBMSCs were cultured in α -MEM medium supplemented with 20% FBS, 1% glutamix 100x, and 1% antibiotic-antimycotic (AA), in a humidified atmosphere containing 5% CO₂. The cells were then seeded at a density 5 \times 10⁴/ml and passaged at 80% confluence. The cultured medium was refreshed every two days. The 3rd passage was used in the experiments that occurred later on.

Cell markers were used to check the phenotype of PBMSCs by flow cytometry. The whole process followed the user's instructions from the manufacturer. It can be briefly described as follows. PBMSCs were seeded on a 15-mm culture plate with a density of 5 \times 10⁶. The cells at 80% confluence were trypsinized with 0.25% Trypsin-EDTA (Gibco) and then washed by PBS for 3 times. The trypsinized PBMSCs were washed with stain buffer (with BSA or PBS) and re-suspended in 10 ml of stain buffer for cell counting. PBMSCs were resuspended in a 1-ml tube (Eppendorf) with a concentration of 106 cells/ml. 100 μ l of stain buffer was added into the 1-ml Eppendorf and then kept at 4 $^{\circ}$ C for 10 min. Subsequently, primary antibodies CD29, CD44 (Sigma, Saint Louis, USA), and CD45 (Bio-Rad) were added into the tube and incubated for 45 min on ice without light exposure. The cells were washed twice using stain buffer; and followed to apply the goat anti-mouse IgG (H + L) (Sigma) as the secondary antibody and incubated for another 45 min. Finally, the cells were re-suspended in 500 μ l stain buffer and transferred to the new strainer tube before FACS scan in flow cytometry (Beckman Coulter FC500).

2.10. Evaluation of stemness or multilineage potentials of PBMSCs cultured with prepared PRPs

For the evaluation of chondrogenesis potential, the PBMSCs were seeded on a 6-well plate with a density of 5 \times 10⁵ cells/well and treated with chondrogenic induction medium as follows: α -MEM supplemented with 20% FBS; 10 ng/ml TGF- β 1; 1:100 ITS premix (Discovery Labware, Inc, USA); and 15 μ M ascorbic acid. After being cultured for one day, the induction medium was replaced by combination cultured medium of 95% α -MEM and 5% prepared PRPs and cultured another 1 week. Alcian Blue Stain was used to check the secretion of sulfated glycosaminoglycans under a confocal microscope; that has a clear description in section 2.11. The gene expressions of AGN, Coll II, and SOX-9 were used to know whether cells could proliferate and keep its phenotype or not; the detailed procedure is described clearly in section 2.12.

To evaluate the adipogenic potential, PBMSCs were cultured under the condition described in the previous paragraph. The cells treated with an adipogenic induction medium are as follows: α -MEM supplemented with 10% FBS; 1 μ M dexamethasone; 0.5 mM isobutyl-methylxanthine (IBX); 10 μ g insulin; and 100 μ g/ml indomethacin. After being cultured for one day, the induction medium was replaced by a combination cultured medium of 95% α -MEM and 5% prepared PRPs and cultured for another week. Oil Red O staining was used to check the oil drop formation in the cytoplasm under a confocal microscope; that has a clear description in section 2.11. AP2, LPL, and PPAR- γ 2 were used to check the adipo-gene expressions; the detail procedure is described

clearly in section 2.12.

To evaluate the osteogenic potential, PBMSCs were cultured in the same condition as the previous description. The cells treated with an osteogenic induction medium are as follows: α -MEM supplemented with 10% FBS; 0.1 μ M dexamethasone (Sigma), 5 mM β -glycerophosphate (sigma); and 50- μ M ascorbic acid (sigma). After being cultured for one day, the induction medium was replaced by a combination cultured medium of 95% α -MEM and 5% prepared PRPs and cultured for another 2 weeks. Alizarin Red S stain was used to check the calcium-phosphate deposition in the extracellular matrix under a confocal microscope; a detailed description is in the next section 2.11. ALP, Osteocalcin, and CbFa1 were used to check the osteo-gene expressions; the detailed procedure is described clearly in section 2.12.

2.11. Detection of specific matrix accumulation

The chondrogenic cells were fixed in 3.7% formaldehyde and stained with 0.05% Alcian Blue Solution (1% in 3% acetic acid, pH 2.5, Sigma) and incubated in the dark for 45 min at room temperature. Under the light microscope, the chondrocytes were an intensely blue colour. To quantify chondrocyte differentiation marked by a blue colour from Alcian blue, followed by gradual elution of the bound dye by dissociated solution (8 M Guanidine-HCL solution) for 24 h. The eluted solutions were then measured by using a spectrophotometer at 610 nm.

To quantify the intracellular lipid vesicle of adipogenic differentiation, the fixed cells in 3.7% formaldehyde were stained with 0.5% Oil Red O solution in isopropanol (Sigma) for 15 min. After observing the bright-red stained lipid vesicle formation under a light microscope, the cell-bound staining was completely dissolved with 1 ml absolute isopropanol. The extracted Oil Red O was then assayed spectrophotometrically at 550 nm.

As the osteogenic potential, the fixed cells were stained with Alizarin Red S solution (Sigma), pre-adjusted to pH 5.5 with 0.5% NH₄OH, for 5 min. The bright orange-red stained extracellular calcium depositions were observed by a light microscope. To measure the extracted solution of cell-bound Alizarin Red S, the stained cells were dissolved in 1 ml phosphate buffer (8 mM Na₂HPO₄ + 1.5 KH₂PO₄) containing 10% cetylpyridinium chloride (sigma) for overnight incubation and measured spectrophotometrically at 550 nm.

The expression ratios for specific matrix accumulation of the multi-lineage potential were plotted, where the dissociated solutions were used as the blank group for the baseline check.

2.12. Expression evaluation of differentiated-related genes through RT-PCR

The total RNA was isolated from sub-confluent monolayer cultures with Tri Reagent® (Sigma) according to the manufacturer's instructions and subjected to reverse transcription (RT) followed by PCR amplification for specifically expressed genes. RT was performed with Superscript® III first-strand (Invitrogen Life Technologies, Carlsbad, CA, USA) to convert 0.1 μ g of total RNA. Briefly, 0.1 μ g of each group of RNA was added to bring the final volume to 20 μ L solution containing 50 μ M oligo (dT)20; 10 mM dNTP mix; DEPC-treated water; 10x RT buffer; 25 mM MgCl₂; 0.1 M DTT; RNaseOUTTM (40 U/ μ L); and Superscript® III RT (200 U/ μ L). RNA denature and annealing, and cDNA synthesis were done using a Thermal cycler GeneAtlas Type-E (ASTEC.CO.,LTD). Additionally, 5 ng/ μ L of cDNA was used for PCR amplification (The light cycler 480 system, Roche) in a final volume of 10 μ L containing 5 μ L SYBR Green qPCR Master Mix (2x) (Thermo Scientific); DEPC water; and upstream/downstream primers (Table 3, from MDBio.Inc).

2.13. Statistics

The results are expressed as mean \pm S.D by using GraphPad Prism software 6. The data were analysed by one-way ANOVA, followed by a

Table 3

The Primers designed for RT-PCR in gene expression analysis.

Symbol	Primer sequences (5'→3')	Size (bp)	Annealing Temp. (°C)
<i>GAPDH</i>	GCTTTGCCCGCGATCTAATGTTTC GCCAAATCCGTTCACTCCGACCTT	90	63.1
<i>cbfa1</i>	GAGGAACCGTTTCAGCTTACTG CGTTAACCAATGGCAGCAG	167	63.1
<i>ALP</i>	ATGAGCTCAACCGGAACAA GTGCCCATGGTCAATCCT	131	56
<i>OC</i>	TCAACCCCGACTGCGACGAG TTGGAGCAGCTGGGATGATGG	204	68
<i>AGN</i>	TTCCCTGAGGCCGAGAAC GGGCGGTAATGGAACACAAC	194	65.5
<i>Sox9</i>	CCGGTGGCGTCAAC TGCAGGTGGGGTACTGAT	119	57.5
<i>Col2</i>	CTGGAGCTCCTGGCCTCGTG CAGATGGCCCTTTGGGACCAT	138	67.1
<i>aP2</i>	GGCCAAACCCAACTGA GGGCGCCTCCATCTAAG	167	59.8
<i>PPARγ2</i>	GCGCCCTGGCAAAGCACT TCCACGGAGCGAAACTGACAC	238	59.8
<i>LPL</i>	GCAGGAAGTCTGACCAATAAG GGTTTCTGGATGCCAATAC	183	54.3

Tukey multiple comparison test where significance levels were indicated as *p < 0.05, **p < 0.01, and ***p < 0.001.

3. Results

3.1. The structure and membrane pore size

Fig. 2 shows the structure and the cut-off pore size of the membranes. The pores formed on the membrane spread evenly. However, there is found some large pores sporadically on the membranes, as shown Fig. 2 (A), (B), and Fig. 2(C). Further, the average cut-off pore size of each membrane was close to the product labelling which were $4.89 \pm 0.020 \mu$ m, 2.69 ± 0.001 , and $1.93 \pm 0.006 \mu$ m for the group of H5M, H3M, and H2M, respectively (Fig. 2(D), (E), and Fig. 2(F)). In addition, the illustration informs the most platelets pass through the membrane related to cut-off pore size and parallel to the pores, as shown Fig. 2(G), (H), and Fig. 2(I).

3.2. The platelet concentration of prepared PRPs

As shown in Fig. 3, the platelet concentration of group CP-PRP and group WB were $239 \times 10^3/\mu$ L and $119 \times 10^3/\mu$ L, respectively; which was approximately 2-times rich. The platelet number for group H5M, group H3M, group H2M, group VB, group AP, group SL and group MS are $8.5 \times 10^3/\mu$ L, $17.0 \times 10^3/\mu$ L, $22.0 \times 10^3/\mu$ L, $13.0 \times 10^3/\mu$ L, $6.0 \times 10^3/\mu$ L, $8 \times 10^3/\mu$ L and $19 \times 10^3/\mu$ L, respectively. Among those, the group H2M showed the highest platelet number. Although the platelet concentration of group CP-PRP and group WB was much higher than that of group H2M, CP-PRP contains too many white blood cells (WBCs) that may lead to intensifying of local inflammation; and WB contained large amounts of WBCs and red blood cells (RBCs), as shown in Table 4.

3.3. Cellular characterization of prepared PRPs

Table 4 shows at summary of cellular characterization and concentration of prepared PRPs. The home-designed groups, such as group H5M, group H3M, and group H2M collected relatively high final volume and volume yield of PRPs from the whole blood, compared to that of commercialized kits of group VB and group AP. Group SL showed a high number for final volume and volume yield; however, the platelet number was relatively low. Group MS was as good quality as group H2M in the final volume, volume yield or platelet number.

The group H2M was permeable only for the platelets. Therefore, the

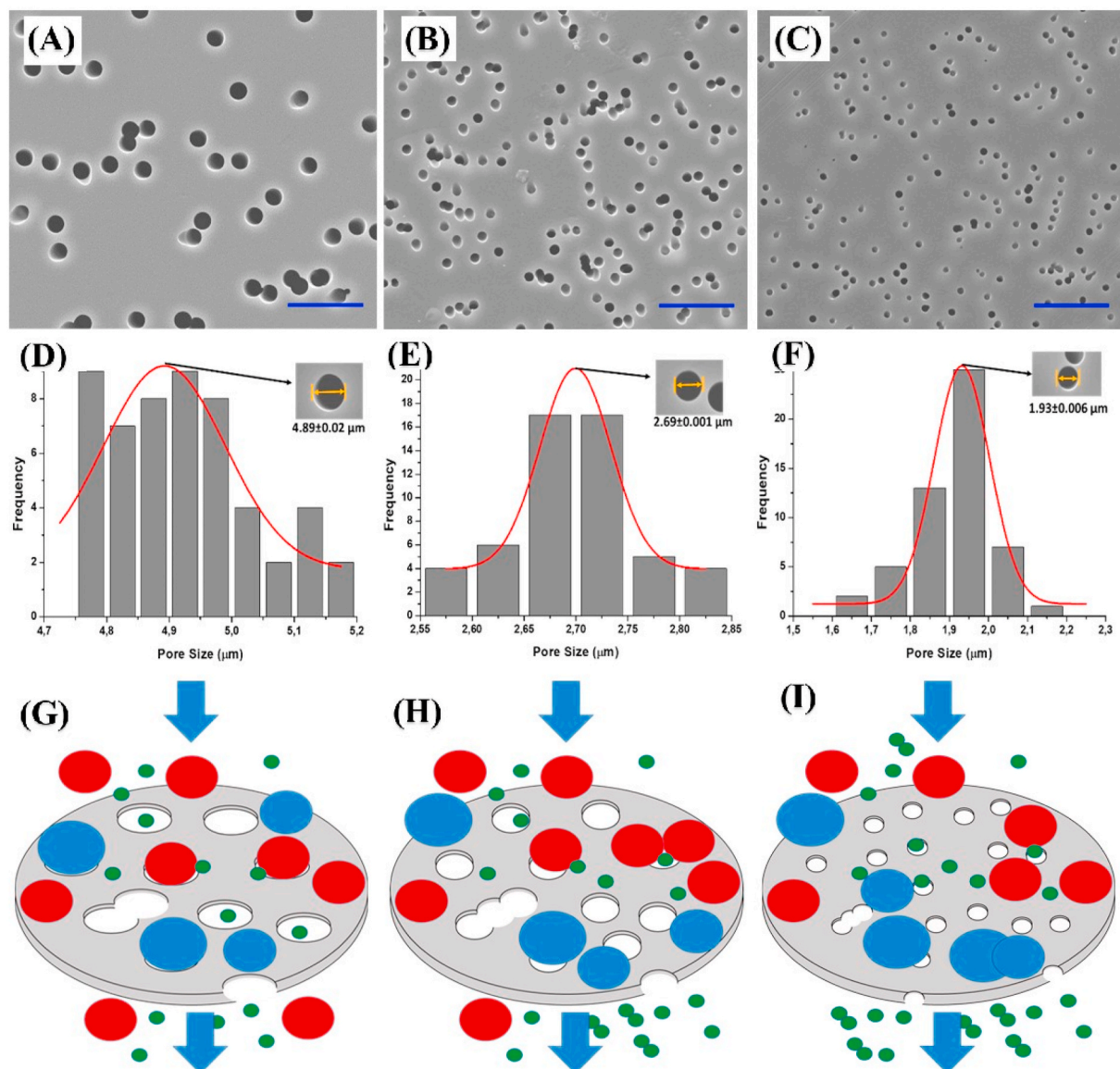


Fig. 2. The structure and morphology of separation membrane for group H5M, group H3M and group H2M were examined under SEM as in (A), (B), and (C), respectively. The (D), (E) and (F) were the average pore size by using Gaussian distribution which is $4.89 \pm 0.02 \mu\text{m}$, $2.69 \pm 0.00 \mu\text{m}$, and $1.93 \pm 0.00 \mu\text{m}$ for H5M, H3M, and H2M, respectively. The (G), (H), and (I) showed how the pore structure separates blood elements based on its size. An angle of 90° or perpendicular between the separation membrane surface and the rotor angle was necessary. The scale bar is $20 \mu\text{m}$.

group H2M had a high relative concentration of platelet increment (RCPI) around 225.09%. The group H5M and group H3M had lower RCPI at 49.69% and 156.18%, respectively, due to contained RBCs. The PRPs prepared by commercial kits all showed maximum RCPI at 225.09% because they were plasma-based kits; thus, its PRP products were free from RBCs and WBCs. Nevertheless, those have lower platelet concentration. The home-designed groups could effectively separate RBCs and WBCs from PRPs, especially for the H2M group. Even though the H5M and H3M could reduce the RBCs to 0.13% and 0.17%, respectively, compared to the CP group.

From the results of Fig. 3 and Table 4, we can tell that the PPRs prepared from group H2M and group MS had the best performance in blood cell characterizations, such as final volume, volume yield, platelet yield, RBCs, WBCs, RCP and RCPI.

3.4. Growth factor quantification

The growth factor quantification of the prepared PRPs is shown in

Fig. 4. The concentration of four growth factors, FGF-2, TGF β -1, BMP2, and IGF-1 in the PRPs prepared from home-designed groups and the CP group were all far above average. The concentration of growth factors in PRPs prepared from the other commercialized kits fluctuated very much. In FGF-2 (Fig. 4(A)), group H5M, group H3M, group H2M, group AP and group CP were all higher than 750 pg/ml. Group VB, group MS and group SL were lower than 500 pg/ml. Group SL was lower than 200 pg/ml.

In the concentration of TGF β -1 (Fig. 4(B)), group H5M, group H3M, group H2M, and group CP were all higher than 1750 pg/ml. Group VB and group SL were lower than 1500 pg/ml. Group AP and group MS were even lower than 200 pg/ml.

In the quantification of BMP2, the groups H3M, H2M, VB, AP, SL and CP showed no significant difference, as shown in Fig. 4(C). H5M and MS were statistically higher than others, but there was not a large difference in between.

In the part of IGF-1, the groups H3M, H2M, VB, AP, MS, SL, and CP showed no significant difference in IGF-1 concentration, which was

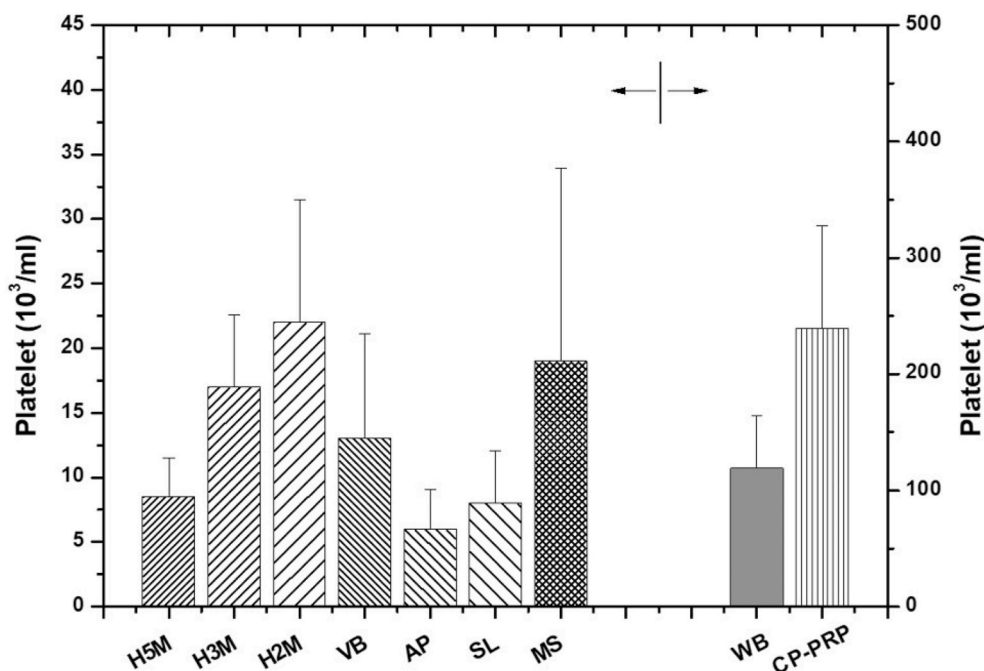


Fig. 3. The number of platelets of prepared PRPs from home-designed kit PRPs, commercialized kit PRPs, whole blood (WB), and conventional protocol PRP (CP-PRP).

Table 4

Comparison of the cellular characteristics and variation of PRP prepared for homemade designs and commercial kits.

PRP kits	Initial volume (ml)	Final volume (ml)	Volume Yield (VY %)	Platelet Yield (PY %)	RBC Yield (RY %)	WBC Yield (WY %)	Relative concentration on of platelets (RCP %)	Relative concentration of platelet increment (RCPI %)
CP-PRP	30	15.65 ± 1.32	50.24 ± 4.40	100.90 ± 8.83	0.18 ± 0.03	27.83 ± 15.94	71.08	159.99
H5M	4	1.93 ± 0.09	48.13 ± 2.29	3.44 ± 0.16	0.05 ± 0.02	0	22.08	49.69
H3M	4	1.82 ± 0.09	45.39 ± 2.37	6.48 ± 0.34	0.01 ± 0.00	0	69.39	156.18
H2M	4	1.82 ± 0.09	45.39 ± 2.37	8.39 ± 0.44	0	0	100	225.09
VB	10	3.833 ± 0.29	38.33 ± 1.44	4.19 ± 0.16	0	0	100	225.09
AP	10	4.40 ± 0.26	43.98 ± 1.31	2.22 ± 0.07	0	0	100	225.09
SL	8	3.83 ± 0.30	47.92 ± 1.80	3.22 ± 0.12	0	0	100	225.09
MS	10	5 ± 0.50	50 ± 2.50	7.98 ± 0.40	0	0	100	225.09

higher than 40 ng/ml in all the groups as shown in Fig. 4(D). H5M was lower than 30 ng/ml which was lower than the other groups.

The results demonstrate that the concentration of growth factors in group H3M, group H2M, and group CP are relatively stable and far above average.

3.5. Structure of fibrin network from prepared PRP

The different fibrin scaffolds were prepared by activating PRPs from different home designed or commercialized kits with calcium chloride. After clot formation, the morphological analysis of the fibrin scaffolds was examined under SEM. As shown in Fig. 5, the fibrin network structure was basically composed of different sizes of fibrils cross-linked by fibrinogen. All the fibrils were linked together as strands or strings that turned into an inter-connected porous structure for nutrient transportation. For all the PRP groups in the study, there was no significant difference in fibrin network structure such as pore size, porosity, diameter, distribution of fibrils and morphology of the scaffold.

3.6. The evaluation of cell viability

In the study, the cell viability was evaluated by WST-1 assay which followed the guidance of ISO-10993 as shown in Fig. 6. The cell viability for group H2M, group AP, group SL, and group MS were all higher than 150%. The cell viability for group H5M, group H3M, and group VB was between 125% and 140%. The cell viability of group CP-PRP was a little bit lower than 100%.

3.7. The results of live/dead stain

Fig. 7 shows the results of Live/Dead stain for all the groups. The green colour was living cells, and the red colour showed the dead cells. We could tell there was no statistical difference in the living and dead cells for all the groups when compared to a controlled group. CP-PRP showed higher red number which was due to RBCs and WBCs contained in the PRP.

3.8. PBMSCs multilineage potential

CD29, CD44, and CD45 were the cell surface markers used to

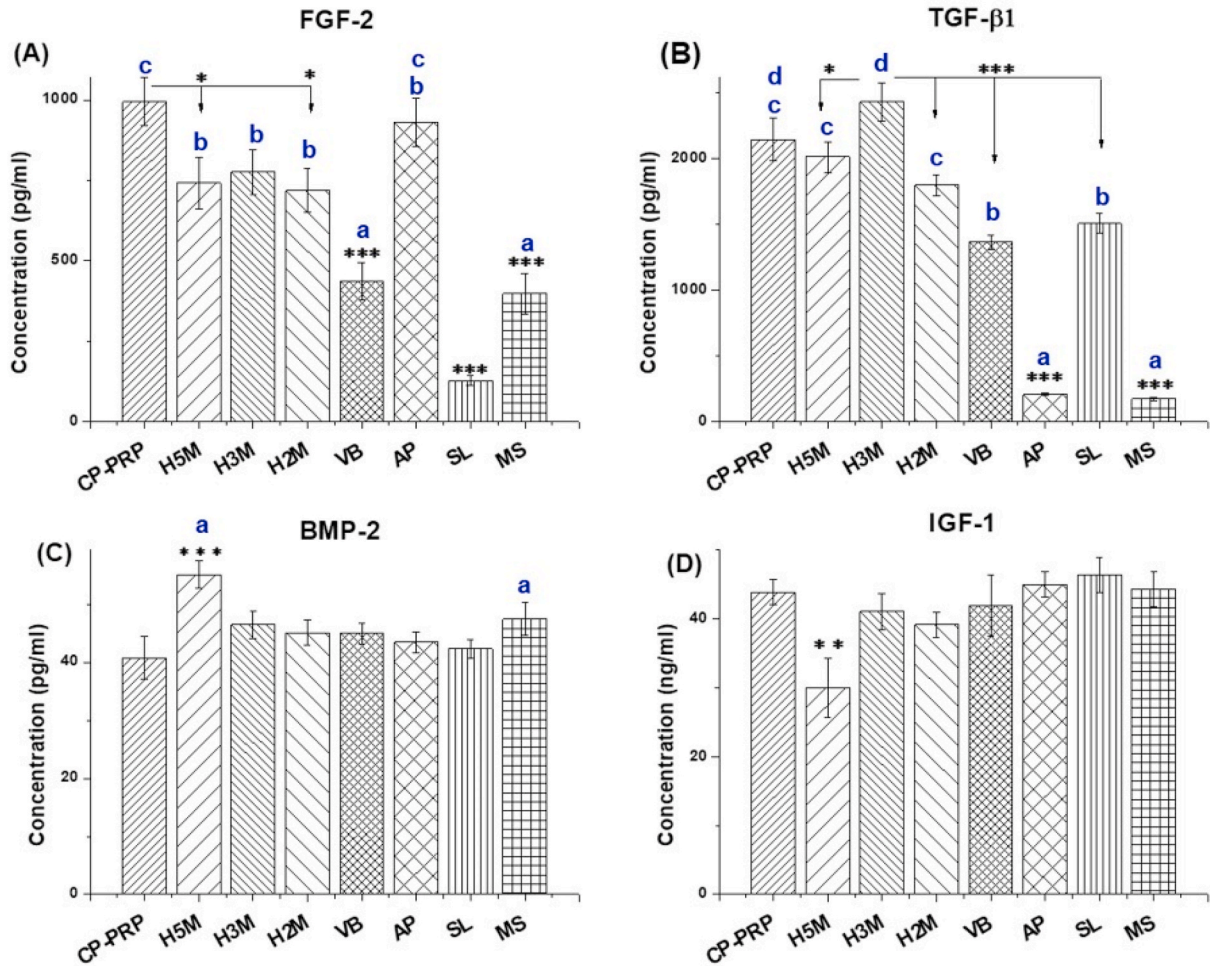


Fig. 4. Growth factor released from activated PRPs (A) FGF-2, (B) TGF-β1, (C) BMP-2, and (D) IGF-1, wherein the same letter mark of a, b, c, d, or d means no significant difference, and significance levels were indicated as * ($p < 0.05$), ** ($p < 0.01$), and *** ($p < 0.001$).

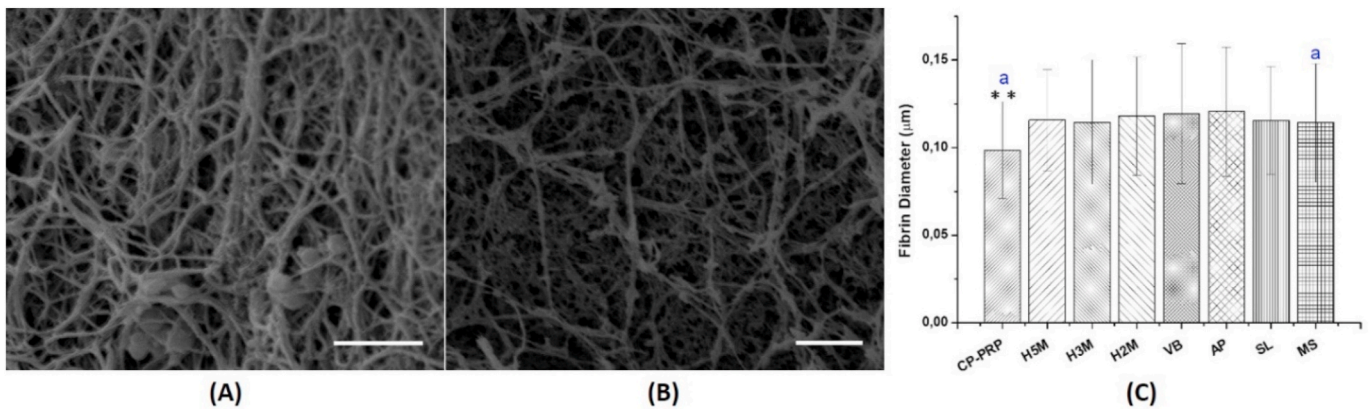


Fig. 5. SEM examination of fibrin structures of PRPs activated by CaCl₂, (A) the fibrin network structure of CP-PRP, (B) close examination of bridging strands and strings of CP-PRP, (C) the average of fiber size for all the PRPs. The same mark a means no significant difference, and significance levels were indicated as ** ($p < 0.01$). The scale bar is 3 μm.

characterize the third passage of isolated PBMSCs. As shown in Fig. 8, PBMSCs all presented CD29⁺, CD44⁺ and CD45⁻ in cell marker analysis under flow cytometry. The characterized PBMSCs were used for the later experiments on the evaluation of stemness and multiple potentials.

The PBMSCs were converted to chondrocytes using a chondrogenic induction medium: α-MEM supplemented with 20% FBS; 10 ng/ml TGF-

β1; 1:100 ITS premix (Discovery Labware, Inc, USA); and 15 μM ascorbic acid. Fig. 9(A) shows the gene expressions of AGN, COL2, and SOX9 to identify the chondrogenic potential. The baseline was the PBMSCs cultured with medium without the addition of PRP. H2M had the highest value of AGN and the rest of the groups were very close to the baseline. In COL2 gene expression, group VB showed the highest AGN value. The

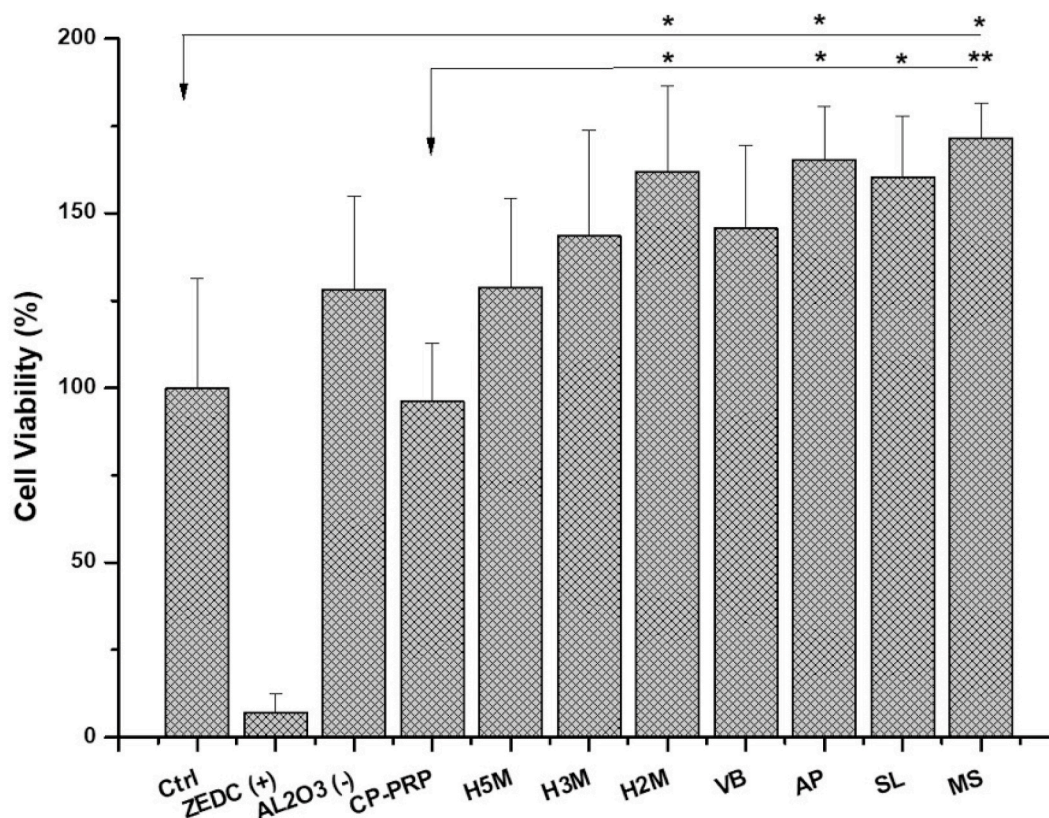


Fig. 6. The cell viability of all the PRPs groups to follow the regulation of ISO-10993 by WST-1 assay. and significance levels were indicated as * $p < 0.05$ and **($p < 0.01$).

rest of the groups showed no significant differences in COL2 expression. The gene expressions of SOX9, group H5M, group H2M, group VB and group MS were all higher than fold 15.75. The other groups, though, were not so high. They were all much higher than the baseline.

The PBMSCs were converted to adipocytes using an adipogenic induction medium: α -MEM supplemented with 10% FBS; 1 μ M dexamethasone; 0.5 mM isobutyl-methylxanthine (IBX); 10 μ g insulin; and 100 μ g/ml indomethacin. Fig. 9(B) shows the gene expression of aP2, LPL and PPAR γ 2 to check the adipogenic potential. In the expression of aP2 gene, group H2M, group VB, and group AP were higher than fold 2.2; the rest of the groups were close to the baseline. In the gene expression of LPL, group H2M and group VB were higher than 0.8; the rest were all higher than the baseline. In the expression of PPAR γ 2, group H5M, group H3M, group AP and group CP-PRP were higher than 1.22.

The PBMSCs were converted to osteoblasts using an osteogenic induction medium: α -MEM supplemented with 10% FBS, 0.1 μ M dexamethasone (Sigma), 5 mM β -glycerophosphate (sigma); and 50- μ M ascorbic acid (sigma). Fig. 9(C) shows the gene expression of ALP, OC and cbfa1 to check the adipogenic potential. Group H5M and group MS had higher expression of ALP. Group SL showed the highest value in OC expression. Group H5M, group H3M, group H2M and group SL were all higher than 24 in cbfa1 expression.

Generally speaking, the PBMSCs cultured in the medium with the addition of PRP for a period of time showed that the relative gene expressions for the test groups were all higher than the baseline. From the results, we believe that PBMSCs could keep stemness and multi-differentiation potentials in chondrogenesis, adipogenesis, and osteogenesis.

In this study, we used a histo-immuno stain to further check the multi-lineage potentials of the PBMSCs cultured with prepared PRPs by using Alcian Blue, Oil Red O and Alizarin Red S to confirm the potential of

chondrogenesis, adipogenesis, and osteogenesis, respectively, as shown in Fig. 10. The results showed that all the test groups were in positive stain to keep the multi-differential potentials.

4. Discussion

As is known, blood elements are different in size and diameter. The platelet is around 2–3 μ m, erythrocytes are about 6–9 μ m and leukocytes are approximately 6–19 μ m [29–32]. The home-designed tube has a membrane with a proper pore size in the middle of a centrifuge-tube to serve as a filter, which is used to separate the platelet and plasma from the erythrocytes & leukocytes that the last-two mentioned may not only induce local inflammation but also slow down the healing process. The group H5M and H3M have a membrane with a cut-off pore size of 5 μ m and 3 μ m, respectively, in the middle of the tube. Supposedly, H5M and H3M could easily separate white blood cells from the final PRP product. However, the white blood cells had an extremely low concentration of PRPs when prepared by the H5M and H3M tubes. The WBCs could be traced sporadically in some of PRPs samples. Charged particles are used to create cut-off pore size in the polycarbonate membrane; but the accelerated heavy ions penetrate into the membrane sometimes are too close or not parallel to each other which may leave many larger pores on the membrane as shown in Fig. 2. Although the average pore size of H5M and H3M is close to 5 μ m and 3 μ m, the larger blood particles such as WBCs could pass through the separating pores which might be due to (1) stress from the high-speed of centrifugation which allows the soft cells to squeeze through the pores, and (2) the close charged-particle beams irradiated on membrane and increased exposure time during etching could be the aspect widen the tract into full-fledged pores, thus it creates unexpected larger pores that allow WBCs to go through [30].

Besides, the cut-off pore size is only one of the selective factors in determining the final number of platelets for a homemade design; the

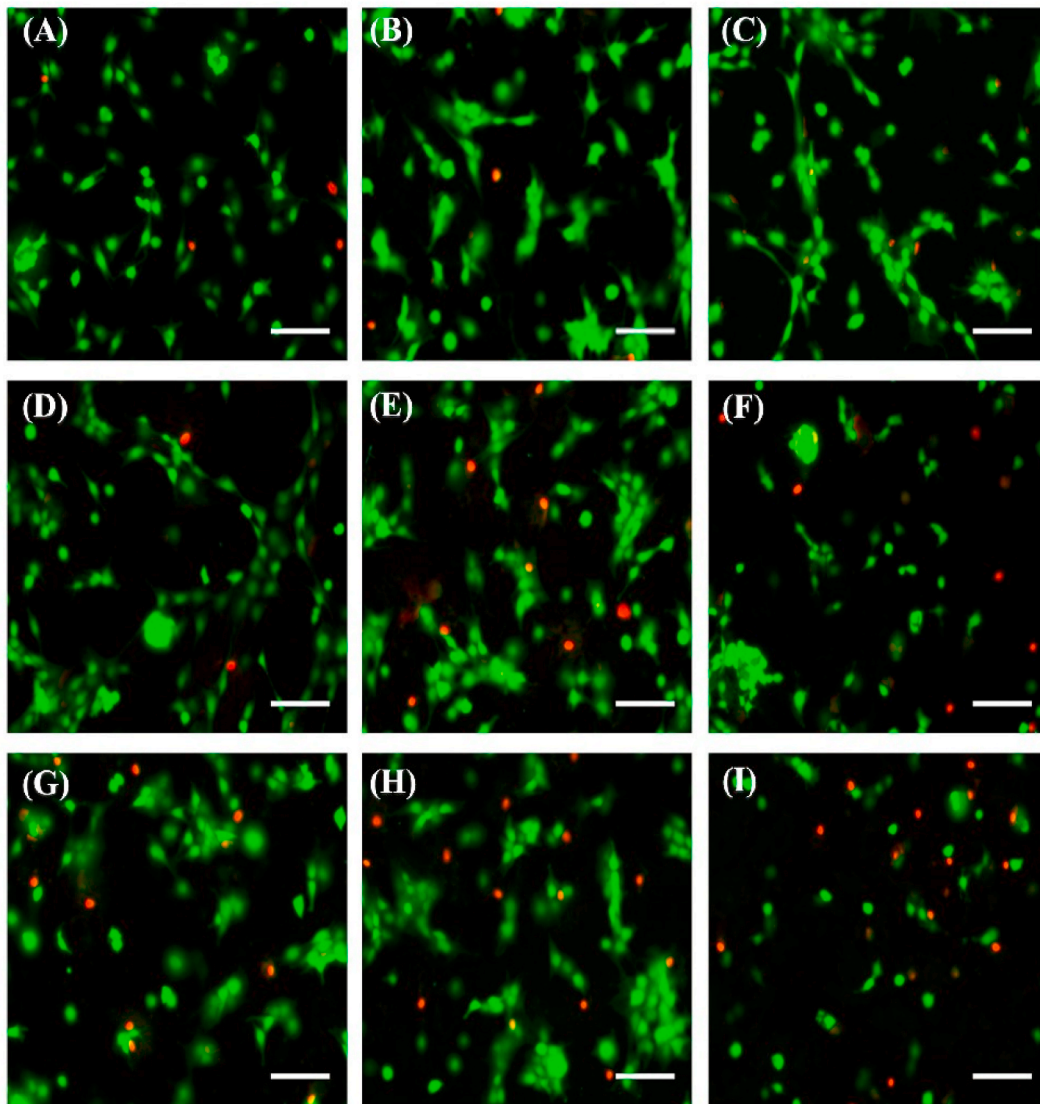


Fig. 7. Live/Dead staining to be in terms of cytotoxicity, (A) Control, (B) H5M, (C) H3M, (D) H2M, (E) VB, (F) AP, (G) SL, (H) MS, and (I) CP-PRP. The scale bar is 150 μ m.

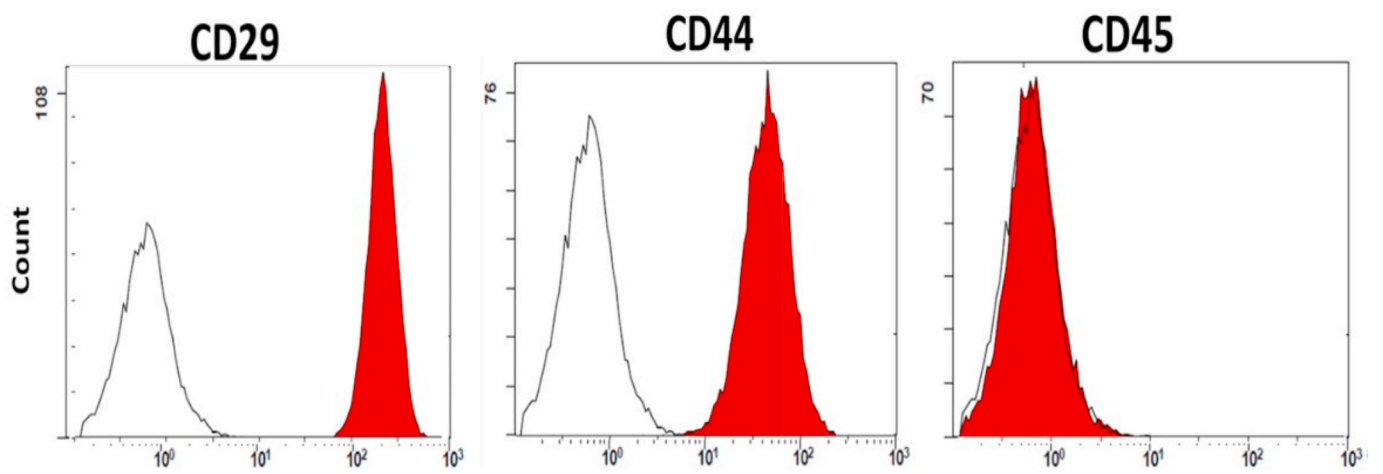


Fig. 8. Immunophenotypic analysis of PBMMSCs at 3rd passage by flow cytometry. The part of the graph in white represents isotype control.

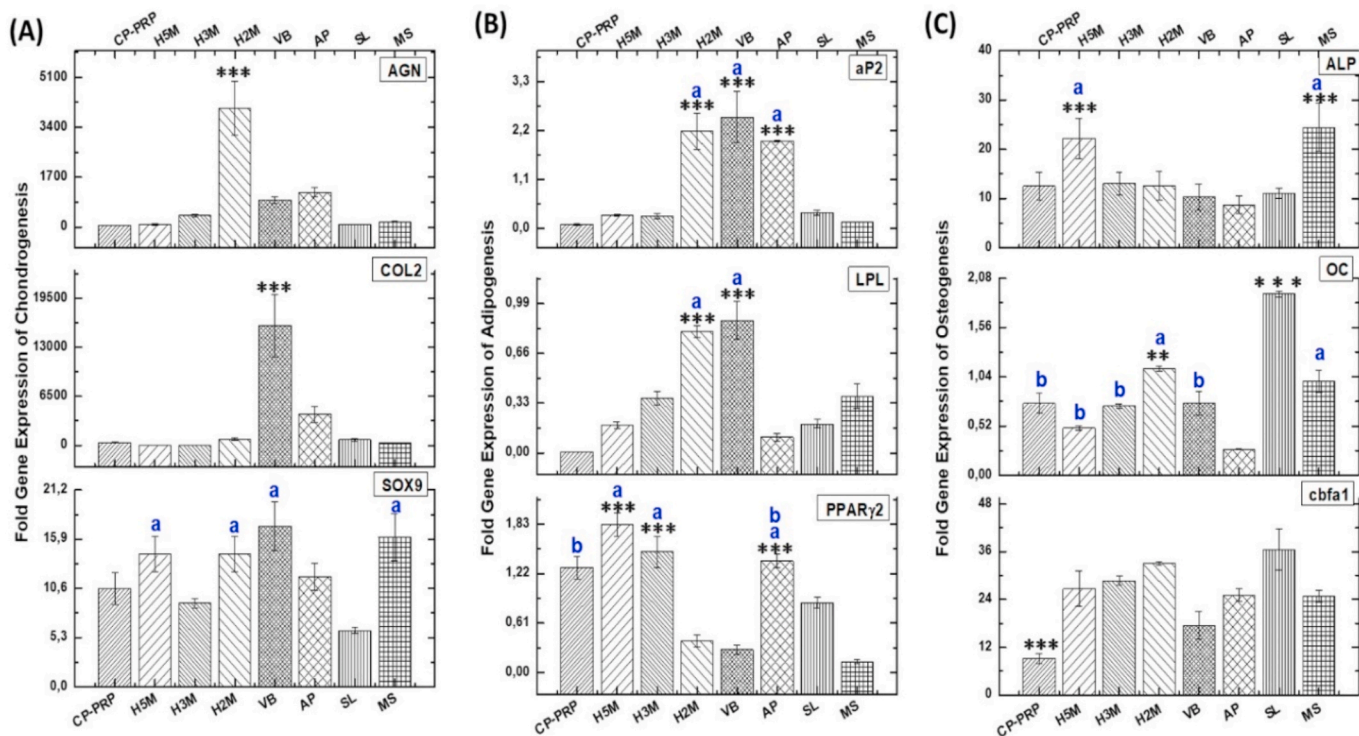


Fig. 9. The evaluation of PBMMSCs multiple potentials by, (A) Chondrogenic-specific genes including aggrecan (AGN), type II collagen (Col2), and SOX9; (B) Adipogenic-specific genes including adipocyte protein 2 (ap2), LPL, and PPAR γ 2; and (C) Osteogenic-specific genes including alkaline phosphate (ALP), osteocalcin (OC), and core-binding factor subunit alpha-1 (cbfa1). GAPDH served as house-keeping gene. The results are shown as three independent experimental, and the same letter mark of a or b means no significant difference, and significance levels were indicated as ** ($p < 0.01$), and *** ($p < 0.001$).

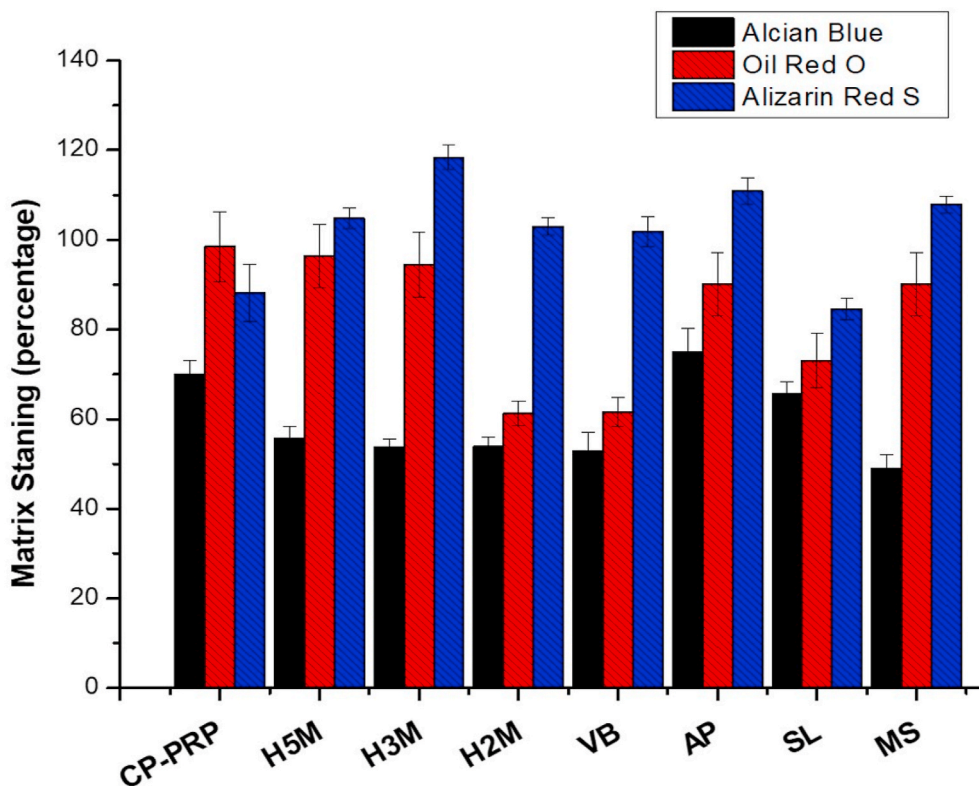


Fig. 10. The quantification of PBMMSCs multilineage differentiation potential by histo-immuno stain of Alcian Blue, Oil Red O and Alizarin Red S to confirm the potential of chondrogenesis, adipogenesis and osteogenesis, respectively.

angle between the rotor angle and the separation membrane was another decisive factor. As illustrated in Fig. 2(G), (H), and Fig. 2(I), most pores formed on the separation membrane were perpendicular to the surface, so that during centrifugation, the flow direction of platelets when striking the separation membrane were parallel to the pores. Therefore, the angle of 90° or perpendicular between the separation membrane surface and the rotor angle was an appropriate consideration.

The average concentration of growth factors released from activated platelets is related to the types and amount of activator used. In previous studies, scientists used different concentrations of CaCl₂, generally between 50 mM–100 mM. If too much CaCl₂ is used as an activator in PRPs, there might be too much Ca⁺² in the PRP matrix to make PBMSCs move toward osteogenesis pathway or could prevent them from maintaining phenotype during proliferation [39–41]. In this study, we used 23 mM of the relatively lower concentration of CaCl₂ as a PRP activator to prevent PBMSCs from undergoing un-desired differentiation during proliferation. Fortunately, this amount of CaCl₂ for PRP activation could produce 80% more growth factors than from the 100 mM activator, as the previous report from Textor et al. states [8].

Platelets and fibrinogen play an essential role in the coagulation process during haemostasis. Activated platelets will induce a fibrinogen monomer to convert into a fibrin polymer with bridging strands or strings of network structure, that could serve as a good framework or matrix for regenerative cell migration, as shown in Fig. 5. The polymerization of fibrinogen, network structure or diameter of the bridging stands was blocked by blood elements contained in the PRPs [16, 42–44]. The CP-PRP shown has a less dense fibrin structure with a flimsy branching network and smaller fibrin size (0.098 ± 0.03 μm) when compared to the other PRP groups, which might be partially due to higher blood elements in the CP-PRP.

The platelets in the PRPs serve as a reservoir for growth factor release which may give nutrients to cells for cell proliferation and cell viability [45–47]. As Fig. 6 shows, the cell viability, which could be in terms of cell number, for all the test groups were much higher than the control group. Platelet-rich plasma (PRP) contains multiple growth factors, such as platelet-derived growth factor, transforming growth factor beta, epidermal growth factor, vascular endothelial growth factor, and fibroblast growth factor, and has been demonstrated to promote the proliferation of BMSCs and ASCs in vitro and improve the overall graft survival *in vivo* [48,49]. The results of Fig. 6 are in agreement with that of Fig. 7. The results tell us that the effect of PRPs on PBMSCs will promote proliferation and increase cell viability [50,51].

PRP contains high levels of diverse growth factors which can stimulate the proliferation of undifferentiated stem cells, as reported by Lai et al. who say that the proliferation of human adipose stem cells (hASCs) can be induced by PRP via multiple signalling pathways such as ERK1/2, Akt, and JNK [52]. From the results of gene expressions to check multiple linkage potentials, the PBMSCs cultured in medium with PRP addition for a period of time showed that the relative gene expressions for the test groups were all higher than the baseline. We believe that PBMSCs cultured with a PRPs-supplement medium could keep stemness and multi-differentiation potentials in chondrogenesis, adipogenesis and osteogenesis [49].

5. Conclusions

In this study, a home-design PRP device was successfully developed; which used a separation membrane with adequate cut-off pore size, placed it in the middle of the centrifuge tube, and effectively filtered out the RBCs and WBCs from the final PRP product. The cut-off pore size was designed as 5 μm, 3 μm and 2 μm for the groups of H5M, H3M and H2M, respectively. Among those, the home-design H2M showed very promising results no matter the final volume (1.82 ± 0.09 ml), platelet yield (8.39 ± 0.44%), RBCs (0%), WBCs (0%), RCPI value (225.09%), and multiple lineage potential. From the previous evaluation and analysis, the group H2M might not be listed as the best number or values for all

indications; but it was listed in the best and good level for all the tests, when compared with the PRPs prepared from commercialized kits. We believe that group H2M could have great potential to develop into the final product to serve in clinics to match the requirements of first-line clinical people.

Author contributions

SJ: Conceived and designed the study, Investigation, Visualization, Writing-Original Draft, Funding acquisition; TCL, YJS, and MT: Investigation; SCW, YHW and LXL: Reviewed and edited the manuscript; FHL: Conceptualization, Supervision, Writing-Review & Editing. All the authors have read and agreed to the published version of the manuscript.

Funding

This work was supported by the Indonesia Endowment Fund for Education (LPDP) within the ministry of Finance, Indonesia (grant number PRJ-317/LPDP.3/2016).

CRedit authorship contribution statement

Subhaini Jakfar: Methodology, Investigation, Visualization, Formal analysis, Writing – original draft, Funding acquisition. **Tzu-Chieh Lin:** Investigation. **Shinn-Chih Wu:** Resources, Writing – review & editing. **Yao-Horn Wang:** Resources, Writing – review & editing. **Yu-Jun Sun:** Investigation. **Minal Thacker:** Investigation. **Li-Xin Liu:** Writing – review & editing. **Feng-Huei Lin:** Conceptualization, Methodology, Formal analysis, Writing – review & editing, Supervision, All the authors have read and agreed to the published version of the manuscript.

Declaration of competing interest

The authors declare no conflict of interest.

References

- [1] A. Panda, S. Kumar, A. Kumar, R. Bansal, S. Bhartiya, Fibrin glue in ophthalmology, *Indian J. Ophthalmol.* 57 (5) (2009) 371–379.
- [2] W.D. Spornitz, Fibrin sealant: past, present, and future: a brief review, *World J. Surg.* 34 (4) (2010) 632–634.
- [3] K.S. Vyas, S.P. Saha, Comparison of hemostatic agents used in vascular surgery, *Expert Opin. Biol. Ther.* 13 (12) (2013) 1663–1672.
- [4] C.H. Chou, W.T. Cheng, T.F. Kuo, J.S. Sun, F.H. Lin, J.C. Tsai, Fibrin glue mixed with gelatin/hyaluronic acid/chondroitin-6-sulfate tri-copolymer for articular cartilage tissue engineering: the results of real-time polymerase chain reaction, *J. Biomed. Mater. Res.* 82 (3) (2007) 757–767.
- [5] X. Wang, Y. Zhang, J. Choukroun, S. Ghanaati, R.J. Miron, Behavior of gingival fibroblasts on titanium implant surfaces in combination with either injectable-PRF or PRP, *Int. J. Mol. Sci.* 18 (2) (2017).
- [6] D.H. Kim, Y.J. Je, C.D. Kim, Y.H. Lee, Y.J. Seo, J.H. Lee, Y. Lee, Can platelet-rich plasma Be used for skin rejuvenation? Evaluation of effects of platelet-rich plasma on human dermal fibroblast, *Ann. Dermatol.* 23 (4) (2011) 424–431.
- [7] J. Fitzpatrick, M.K. Bulsara, P.R. McCrory, M.D. Richardson, M.H. Zheng, Analysis of platelet-rich plasma extraction: variations in platelet and blood components between 4 common commercial kits, *Orthop J Sports Med* 5 (1) (2017), 2325967116675272.
- [8] J.A. Textor, F. Tablin, Activation of equine platelet-rich plasma: comparison of methods and characterization of equine autologous thrombin, *Vet. Surg. : Vysokomol. Soedin.* 41 (7) (2012) 784–794.
- [9] P. Gentile, J.P. Cole, M.A. Cole, S. Garcovich, A. Bielli, M.G. Scioli, A. Orlandi, C. Insalaco, V. Cervelli, Evaluation of not-activated and activated PRP in hair loss treatment: role of growth factor and cytokine concentrations obtained by different collection systems, *Int. J. Mol. Sci.* 18 (2) (2017).
- [10] D. Fufa, B. Shealy, M. Jacobson, S. Kevy, M.M. Murray, Activation of platelet-rich plasma using soluble type I collagen, *J. Oral Maxillofac. Surg. : official journal of the American Association of Oral and Maxillofacial Surgeons* 66 (4) (2008) 684–690.
- [11] T.N. Castillo, M.A. Pouliot, H.J. Kim, J.L. Dragoo, Comparison of growth factor and platelet concentration from commercial platelet-rich plasma separation systems, *Am. J. Sports Med.* 39 (2) (2011) 266–271.
- [12] G. Fernandes, S. Yang, Application of platelet-rich plasma with stem cells in bone and periodontal tissue engineering, *Bone Res* 4 (2016) 16036.
- [13] C.E. Martinez, R. Gomez, A.M. Kalergis, P.C. Smith, Comparative effect of platelet-rich plasma, platelet-poor plasma, and fetal bovine serum on the proliferative

- response of periodontal ligament cell subpopulations, *Clin. Oral Invest.* 23 (5) (2019) 2455–2463.
- [14] D.J. Sanchez-Gonzalez, E. Mendez-Bolina, N.I. Trejo-Bahena, Platelet-rich plasma peptides: key for regeneration, *Int J Pept* 2012 (2012) 532519.
- [15] S. Kushida, N. Kakudo, N. Morimoto, T. Hara, T. Ogawa, T. Mitsui, K. Kusumoto, Platelet and growth factor concentrations in activated platelet-rich plasma: a comparison of seven commercial separation systems, *J. Artif. Organs : the official journal of the Japanese Society for Artificial Organs* 17 (2) (2014) 186–192.
- [16] D.M. Dohan Ehrenfest, L. Rasmusson, T. Albrektsson, Classification of platelet concentrates: from pure platelet-rich plasma (P-PRP) to leucocyte- and platelet-rich fibrin (L-PRF), *Trends Biotechnol.* 27 (3) (2009) 158–167.
- [17] A. Aguirre, H. Arbildo, J. Peralta, Comparative performance of the protocol of plasma rich in growth factors - universal 1 (PRGF-U1) for obtaining platelet rich plasma, *Journal of Oral Research* 6 (1) (2017) 16–18.
- [18] J.M. DeLong, K. Beitzel, A.D. Mazzocca, D. Shepard, B.L. Roller, B.T. Hanypsiak, Update on platelet-rich plasma, *Current Orthopaedic Practice* 22 (6) (2011) 514–523.
- [19] R. Cancedda, S. Bollini, F. Descalzi, M. Mastrogiacomo, R. Tasso, Learning from mother nature: innovative tools to boost endogenous repair of critical or difficult-to-heal large tissue defects, *Frontiers in bioengineering and biotechnology* 5 (2017), 28–28.
- [20] V. Pavlovic, M. Ciric, V. Jovanovic, P. Stojanovic, Platelet Rich Plasma: a short overview of certain bioactive components, *Open Med.* 11 (1) (2016) 242–247.
- [21] W. Yin, X. Qi, Y. Zhang, J. Sheng, Z. Xu, S. Tao, X. Xie, X. Li, C. Zhang, Advantages of pure platelet-rich plasma compared with leukocyte- and platelet-rich plasma in promoting repair of bone defects, *J. Transl. Med.* 14 (2016) 73.
- [22] F. Eisinger, J. Patzelt, H.F. Langer, The platelet response to tissue injury, *Front Med (Lausanne)* 5 (2018) 317.
- [23] P. Everts, K. Onishi, P. Jayaram, J.F. Lana, K. Mautner, Platelet-rich plasma: new performance understandings and therapeutic considerations in 2020, *Int. J. Mol. Sci.* 21 (20) (2020).
- [24] D. Basu, R. Kulkarni, Overview of blood components and their preparation, *Indian J. Anaesth.* 58 (5) (2014) 529–537.
- [25] R. Dhurat, M. Suresh, Principles and methods of preparation of platelet-rich plasma: a review and author's perspective, *J. Cutan. Aesthetic Surg.* 7 (4) (2014) 189–197.
- [26] H.J. Braun, H.J. Kim, C.R. Chu, J.L. Dragoo, The effect of platelet-rich plasma formulations and blood products on human synoviocytes: implications for intra-articular injury and therapy, *Am. J. Sports Med.* 42 (5) (2014) 1204–1210.
- [27] P.A. Everts, G.A. Malanga, R.V. Paul, J.B. Rothenberg, N. Stephens, K.R. Mautner, Assessing clinical implications and perspectives of the pathophysiological effects of erythrocytes and plasma free hemoglobin in autologous biologics for use in musculoskeletal regenerative medicine therapies, A review, *Regen Ther* 11 (2019) 56–64.
- [28] S. Kattula, J.R. Byrnes, A.S. Wolberg, Fibrinogen and fibrin in hemostasis and thrombosis, *Arterioscler. Thromb. Vasc. Biol.* 37 (3) (2017) e13–e21.
- [29] K. Aran, A. Fok, L.A. Sasso, N. Kamdar, Y. Guan, Q. Sun, A. Undar, J.D. Zahn, Microfiltration platform for continuous blood plasma protein extraction from whole blood during cardiac surgery, *Lab Chip* 11 (17) (2011) 2858–2868.
- [30] O.L.O. Božena, A. Sartowska, Presz Adam, I.V.B. Pavel Yu Apel, Nanopores with controlled profiles in track-etched membranes, *Nukleonika* 57 (4) (2012) 575–579.
- [31] P. Noris, C. Klersy, P. Gresele, F. Giona, P. Giordano, P. Minuz, G. Loffredo, A. Pecci, F. Melazzini, E. Civaschi, A. Mezzasoma, M. Piedimonte, F. Semeraro, D. Veneri, F. Menna, L. Ciardelli, C.L. Balduini, P. Italian Gruppo di Studio delle, Platelet size for distinguishing between inherited thrombocytopenias and immune thrombocytopenia: a multicentric, real life study, *Br. J. Haematol.* 162 (1) (2013) 112–119.
- [32] K. Fixter, D.J. Rabbolini, B. Valecha, M.C. Morel-Kopp, S. Gabrielli, Q. Chen, W. S. Stevenson, C.M. Ward, Mean platelet diameter measurements to classify inherited thrombocytopenias, *Int J Lab Hematol* 40 (2) (2018) 187–195.
- [33] C.M. Hawkey, P.M. Bennett, S.C. Gascoyne, M.G. Hart, J.K. Kirkwood, Erythrocyte size, number and haemoglobin content in vertebrates, *British Journal of Haematology* 77 (1991) 392–397.
- [34] M.M. Winer, A. Zeidan, D. Yehezkely-Hayon, L. Golan, L. Minai, E.J. Dann, D. Yelin, In vivo noninvasive microscopy of human leucocytes, *Sci. Rep.* 7 (1) (2017) 13031.
- [35] J. Zhou, C. Tu, Y. Liang, B. Huang, Y. Fang, X. Liang, I. Papautsky, X. Ye, Isolation of cells from whole blood using shear-induced diffusion, *Sci. Rep.* 8 (1) (2018) 9411.
- [36] L. Wiegmann, D.A. de Zélicourt, O. Speer, A. Muller, J.S. Goede, B. Seifert, V. Kurtcuoglu, Influence of standard laboratory procedures on measures of erythrocyte damage, *Front. Physiol.* 8 (2017), 731–731.
- [37] J.E. Mancuso, A. Jayaraman, W.D. Ristenpart, Centrifugation-induced release of ATP from red blood cells, *PLoS One* 13 (9) (2018) e0203270–e0203270.
- [38] S. Arora, V. Doda, U. Kotwal, M. Dogra, Quantification of platelets and platelet derived growth factors from platelet-rich-plasma (PRP) prepared at different centrifugal force (g) and time, *Transfus. Apher. Sci.* 54 (1) (2016) 103–110.
- [39] M.N. Lee, H.-S. Hwang, S.-H. Oh, A. Roshanzadeh, J.-W. Kim, J.H. Song, E.-S. Kim, J.-T. Koh, Elevated extracellular calcium ions promote proliferation and migration of mesenchymal stem cells via increasing osteopontin expression, *Exp. Mol. Med.* 50 (11) (2018) 142.
- [40] F.M.P. Tonelli, A.K. Santos, D.A. Gomes, S.L. da Silva, K.N. Gomes, L.O. Ladeira, R. R. Resende, Stem cells and calcium signaling, *Adv. Exp. Med. Biol.* 740 (2012) 891–916.
- [41] D. Ponnaiyan, V. Jegadeesan, Comparison of phenotype and differentiation marker gene expression profiles in human dental pulp and bone marrow mesenchymal stem cells, *Eur. J. Dermatol.* 8 (3) (2014) 307–313.
- [42] J.W. Weisel, R.I. Litvinov, Fibrin formation, structure and properties, *Subcell. Biochem.* 82 (2017) 405–456.
- [43] M.R. Palvo, O.V. Gorkun, S.T. Lord, The molecular origins of the mechanical properties of fibrin, *Biophys. Chem.* 152 (1) (2010) 15–20.
- [44] E. Pretorius, O.E. Ekpo, E. Smit, Comparative ultrastructural analyses of platelets and fibrin networks using the murine model of asthma, *Exp. Toxicol. Pathol.* 59 (2) (2007) 105–114.
- [45] J. Shen, Q. Gao, Y. Zhang, Y. He, Autologous platelet-rich plasma promotes proliferation and chondrogenic differentiation of adipose-derived stem cells, *Mol. Med. Rep.* 11 (2) (2015) 1298–1303.
- [46] L.B. Navarro, F. Barchiki, W. Navarro Junior, E. Carneiro, U.X. da Silva Neto, V.P. D. Westphalen, Assessment of platelet-rich fibrin in the maintenance and recovery of cell viability of the periodontal ligament, *Sci. Rep.* 9 (1) (2019) 19476.
- [47] D. Steller, N. Herbst, R. Pries, D. Juhl, S.G. Hakim, Positive impact of Platelet-rich plasma and Platelet-rich fibrin on viability, migration and proliferation of osteoblasts and fibroblasts treated with zoledronic acid, *Sci. Rep.* 9 (1) (2019) 8310.
- [48] N. Bertozzi, F. Simonacci, M.P. Grieco, E. Grignaffini, E. Raposio, The biological and clinical basis for the use of adipose-derived stem cells in the field of wound healing, *Ann Med Surg (Lond)* 20 (2017) 41–48.
- [49] M. Tobita, S. Tajima, H. Mizuno, Adipose tissue-derived mesenchymal stem cells and platelet-rich plasma: stem cell transplantation methods that enhance stemness, *Stem Cell Res. Ther.* 6 (2015) 215.
- [50] S. Tavassoli-Hojjati, M. Sattari, T. Ghasemi, R. Ahmadi, A. Mashayekhi, Effect of platelet-rich plasma concentrations on the proliferation of periodontal cells: an in vitro study, *Eur. J. Dermatol.* 10 (4) (2016) 469–474.
- [51] J.Y. Lee, H. Nam, Y.J. Park, S.J. Lee, C.P. Chung, S.B. Han, G. Lee, The effects of platelet-rich plasma derived from human umbilical cord blood on the osteogenic differentiation of human dental stem cells, *In Vitro Cell, Dev Biol Anim* 47 (2) (2011) 157–164.
- [52] F. Lai, N. Kakudo, N. Morimoto, S. Taketani, T. Hara, T. Ogawa, K. Kusumoto, Platelet-rich plasma enhances the proliferation of human adipose stem cells through multiple signaling pathways, *Stem Cell Res. Ther.* 9 (1) (2018) 107.